ACS APPLIED MATERIALS & INTERFACES

Research Article

www.acsami.org

Facile Spray-Coating Process for the Fabrication of Tunable Adhesive Superhydrophobic Surfaces with Heterogeneous Chemical Compositions Used for Selective Transportation of Microdroplets with Different Volumes

Jian Li,* Zhijiao Jing, Fei Zha, Yaoxia Yang, Qingtao Wang, and Ziqiang Lei*

Key Laboratory of Eco-Environment-Related Polymer Materials, Ministry of Education of China, Key Laboratory of Gansu Polymer Materials, College of Chemistry and Chemical Engineering, Northwest Normal University, Lanzhou 730070, China

Supporting Information

ABSTRACT: In this paper, tunable adhesive superhydrophobic ZnO surfaces have been fabricated successfully by spraying ZnO nanoparticle (NP) suspensions onto desired substrates. We regulate the spray-coating process by changing the mass percentage of hydrophobic ZnO NPs (which were achieved by modifying hydrophilic ZnO NPs with stearic acid) in the hydrophobic/hydrophilic ZnO NP mixtures to control heterogeneous chemical composition of the ZnO surfaces. Thus, the water adhesion on the same superhydrophobic ZnO surface could be effectively tuned by controlling the surface chemical composition without altering the surface morphology. Compared with the conventional tunable adhesive superhydrophobic surfaces, on which there were only three different water sliding angle values: lower than 10°, 90° (the water droplet is firmly pinned on the surface at any tilted angles), and the value between the two ones, the water adhesion on the superhydrophobic ZnO surfaces has been tuned effectively, on which the sliding angle is controlled from 2 ± 1° to 9 ± 1°, 21 ± 2°, 39 ± 3°, and 90°. Accordingly, the adhesive force can be adjusted from extremely low (~2.5 μN) to very high (~111.6 μN). On the basis of the different adhesive forces of the tunable adhesive superhydrophobic surfaces, the selective transportation of microdroplets with different volumes was achieved, which has never been reported before. In addition, we demonstrated a proof of selective transportation of microdroplets with different volumes for application in the droplet-based microreactors via our tunable adhesive superhydrophobic surfaces for the quantitative detection of $AgNO_3$ and NaOH. The results reported herein realize the selective transportation of microdroplets with different volumes and we believe that this method would potentially be used in many important applications, such as selective water droplet transportation, biomolecular quantitative detection and droplet-based biodetection.

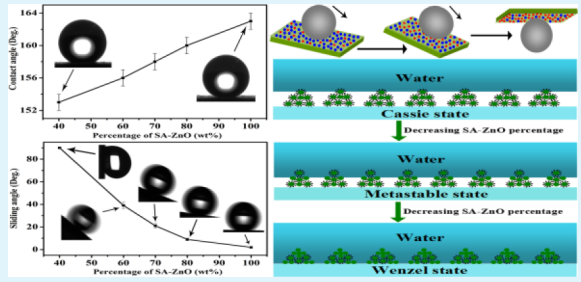

KEYWORDS: *superhydrophobic surfaces, tunable adhesion, selective transportation, heterogeneous chemistry, spray-coating*

1. INTRODUCTION

Superhydrophobic surfaces with a water contact angle (CA) higher than 150° have recently attracted much research attention due to their potential applications in many fields, such as self-cleaning,[1] anticorrosion,[2] antireflection,[3] antifogging,[4] antisticking,[5] anti-icing,[6] oil/water separation,[7] water collection,[8] fluidic drag reduction,[9] and no loss microdroplet transportation.[10] Different requirements need the superhydrophobic surfaces with different adhesions (also reflected by different sliding angle values), because it is the adhesive property that ultimately determines the dynamic action of the liquid on the surface.[11] According to the different water adhesions on the surfaces, superhydrophobic surfaces can be normally classified into two types: low adhesion to water and and high adhesion to water. Low adhesive superhydrophobic surfaces are usually inspired by the lotus leaf.[12] Water on these surfaces almost forms spherical droplets that readily roll away carrying dust and dirt from the surfaces.[13] Recent studies revealed that the low adhesive property of lotus leaves was attributed to the combination of appropriate surface roughness with low surface energy materials.[14] On the other hand, high adhesive superhydrophobic surfaces are inspired by rose petals.[15] On these surfaces, water droplets are firmly pinned without any movement, even when the surfaces were tilted vertically or turned upside down.[16,17] The high adhesive superhydrophobic surfaces are considered to be promising in many potential application, biochemical separation and microfluid systems.[16,18] Recently, particular attention is paid to superhydrophobic surfaces exhibiting tunable water adhesion, because the tunable adhesion allows the manipulation of water droplets on the superhydrophobic surfaces.[19−22] Such tunable adhesive superhydrophobic surfaces are expected to find

Received: March 19, 2014
Accepted: May 8, 2014
Published: May 8, 2014

   dx.doi.org/10.1021/am5015937 | ACS Appl. Mater. Interfaces 2014, 6, 8868−8877

various practical applications in many fields, including no loss microdroplets transportation in fluid-controllable devices,[23] biochemical separation,[24] and microfluidic chips,[25] etc.

It was reported that whether water droplets are pinned on or roll off the superhydrophobic surfaces is attributed to the distinct contact modes: the Cassie state, the metastable state, and the Wenzel state.[11,26,27] In the Cassie state,[28] the water droplet contacts the top of asperities with air trapped at the microscales (dramatic decrease of the surface contact area of the droplet with the microstructure). In this state, the water droplet easily rolls off the surface with extremely low adhesion. Conversely, in the Wenzel state,[29] the water droplet fully wet a textured surface (increase of the surface contact area due to the rough microstructure). Thus, the Wenzel state exhibits an extremely high adhesive property. Additionally, in the metastable state, a water droplet partially wets the roughness features with air trapped in the rest of valleys, thus the adhesion of the surface is between that of the above two states and the water droplet rolls off with the surface significantly tilted.[30,31] In addition, the wettability states may be adjusted between the Cassie state and the Wenzel state via changing the surface chemical composition or surface morphology. Hence, the water adhesion on the superhydrophobic surfaces could be effectively tuned by dynamically controlling the two factors. Inspired by these findings, intensive studies have been focused on design and fabrication of tunable water adhesion on the superhydrophobic surfaces through controlling the surface microstructures.[32−44] For example, Lai et al. designed three types of superhydrophobic TiO_2 porous nanostructures with tunable water adhesion.[32] Li et al. have used a simple-immesion process to prepare superhydrophobic CuO surfaces with tunable water adhesion that ranges from extremely low to very high.[33] Yong et al. realized superhydrophobic patterned polydimethylsiloxane surfaces with controllable water adhesion by a femtosecond laser.[34] In addition to microstructures, chemical composition is another important factor in determining the surface adhesion. It is feasible to achieve tunable water adhesion on superhydrophobic surfaces through adjusting the surface chemical composition. In fact, such research is of great importance not only to help us to further understand the fabrication principle for novel tunable adhesive superhydrophobic surfaces but to design and prepare such superhydrophobic surfaces with tunalbe water adhesion. Up to now, the fabrication of tunable adhesive superhydrophobic surfaces through the control of surface chemical composition without changing the surface microstructure is still scarce.[45−50] Moreover, the water adhesion on the aforementioned superhydrophobic surfaces was not tuned effectively and the water sliding angles on these surfaces were only three different values: lower than 10°, 90°, and the value between the two ones. However, the practical application of manipulating water droplets needs the surfaces with a large range of different sliding angle values (or adhesive property). To the best of our knowledge, the fabrication of superhydrophobic surfaces with extensively tunable adhesion is still scarce.[33]

Herein, through the facile spray-coating process, we fabricated tunable adhesive superhydrophobic ZnO surfaces with a large range of different sliding angle values successfully by varying the composition of hydrophobic and hydrophilic ZnO NPs, and studied the influence of the chemical composition on the water adhesion. In detail, a mixture of hydrophobic ZnO NPs (which were achieved by modifying hydrophilic ZnO NPs with stearic acid, termed as SA-ZnO) and hydrophilic ZnO NPs suspension was sprayed onto the desired substrates to get the superhydrophobic ZnO surfaces with heterogeneous chemical composition (hydrophobic/hydrophilic). The obtained ZnO surfaces show an analogous superhydrophobicity but chemical composition-dependent water adhesion (or water sliding angle). With a decrease of the mass percentage of SA-ZnO NPs in the mixture, the water sliding angle increased from $2 \pm 1°$ to $9 \pm 1°$, $21 \pm 2°$, $39 \pm 3°$, and 90°. Accordingly, the adhesive force between the surface and the water droplet can be adjusted from extremely low (~2.5 μN) to very high (~111.6 μN). On the basis of the different adhesive forces of the tunable adhesive superhydrophobic surfaces, the selective transportation of microdroplets with different volumes was achieved. To the best of our knowledge, it is the first time to use tunable adhesive superhydrophobic surfaces for selective transportation of microdroplets with different volumes. Moreover, the dynamic wetting behavior of a pressed water droplet on the different adhesive superhydrophobic surfaces is demonstrated, and the wetting transition between superhydrophobicity and hydrophilicity cannot or can be achieved on the tunable adhesive superhydrophobic surfaces, depending on the adhesive property of the surfaces, which is determined by the density of the hydrophilic hydroxyl group on the ZnO surfaces. In addition, we demonstrated a proof of selective transportation of microdroplets with different volumes for application in the droplet-based microreactors via our tunable adhesive superhydrophobic surfaces for the quantitative detection of $AgNO_3$ and NaOH. Furthermore, the spray-coating process show advantages of convenience, industrialization and repairability.[51,52] The superhydrophobicity and adhesive property of the damaged superhydrophobic surfaces could be regenerated simultaneously more than once by spraying the mixture ZnO NP suspensions onto the wrecked surfaces. The method used here not only provides a novel strategy to prepare tunable adhesive superhydrophobic surfaces, but also potentially be used in selective transportation microdroplets with different volumes, and we believe that this method is of great importance not only for fundamental research but for various practical applications in biomolecular detection, chemical microreactors and quantitative transportation in biochips.

2. EXPERIMENTAL SECTION

Materials. ZnO NPs were purchased from NanoTek and used as received. Stearic acid and absolute ethanol were obtained from Tianjin Chemical Reagent Co., Ltd. and used without additional purification.

Preparation of the Hydrophobic ZnO NPs. The hydrophobic ZnO NPs were prepared according to our previous reported literature.[43] In brief, hydrophilic ZnO NPs (0.5 g) were dispersed in 0.02 M stearic acid ethanol solution (50 mL) under stirring for 3 h to impart octadecyl groups on their surfaces. After wash and filtration steps, the obtained hydrophobic ZnO NPs were dried and ground to a fine powder.

Preparation of the Superhydrohobic ZnO Surfaces with Tunable Water Adhesion. In a typical process, ZnO NPs (the mass percentage of hydrophobic ZnO NPs in the mixture was changed from 100 to 40 and the whole weight of the mixture is fixed at 0.4 g) were first dispersed in 20 mL of ethanol solution under stirring for 30 min to gain a homogeneous suspension. The suspension was then sprayed onto desired substrates with 0.2 MPa nitrogen gas using a spray gun. Finally, the coating was dried at ambient temperature for 1 h to allow the ethanol to evaporate completely.

Characterization. Fourier transform infrared (FT-IR) spectroscopy was performed with a Bio-Rad FTS-165 instrument. The XRD pattern was carried out on a X-ray diffractometer (Rigaku Corp., D/

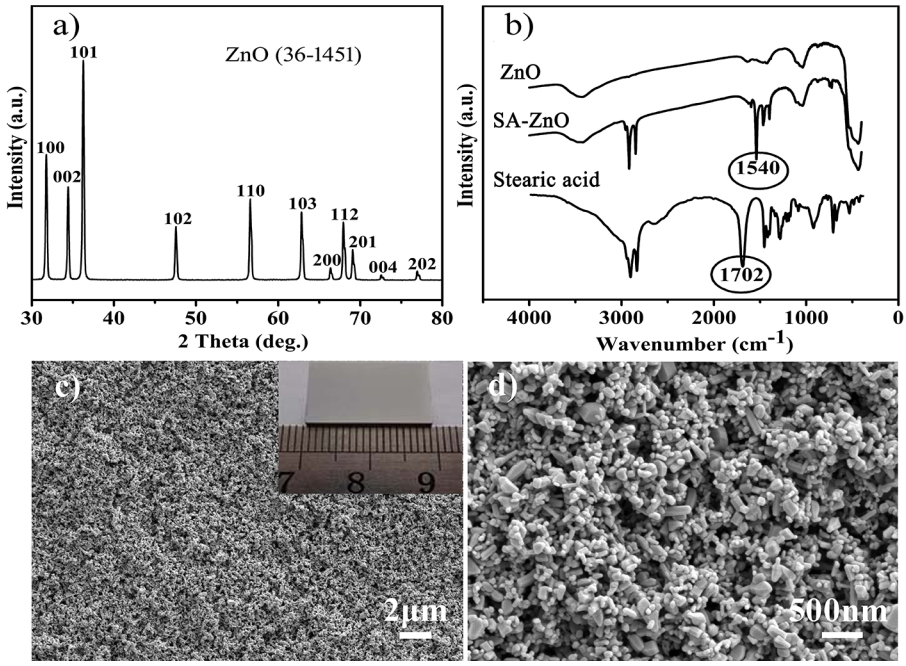

Figure 1. (a) XRD pattern of the as-prepared ZnO surfaces. (b) FT-IR spectra of ZnO, SA-ZnO, and stearic acid. (c,d) FE-SEM images of the as-prepared ZnO surfaces at low and high magnifications. The inset shows the photograph of the as-prepared ZnO surface.

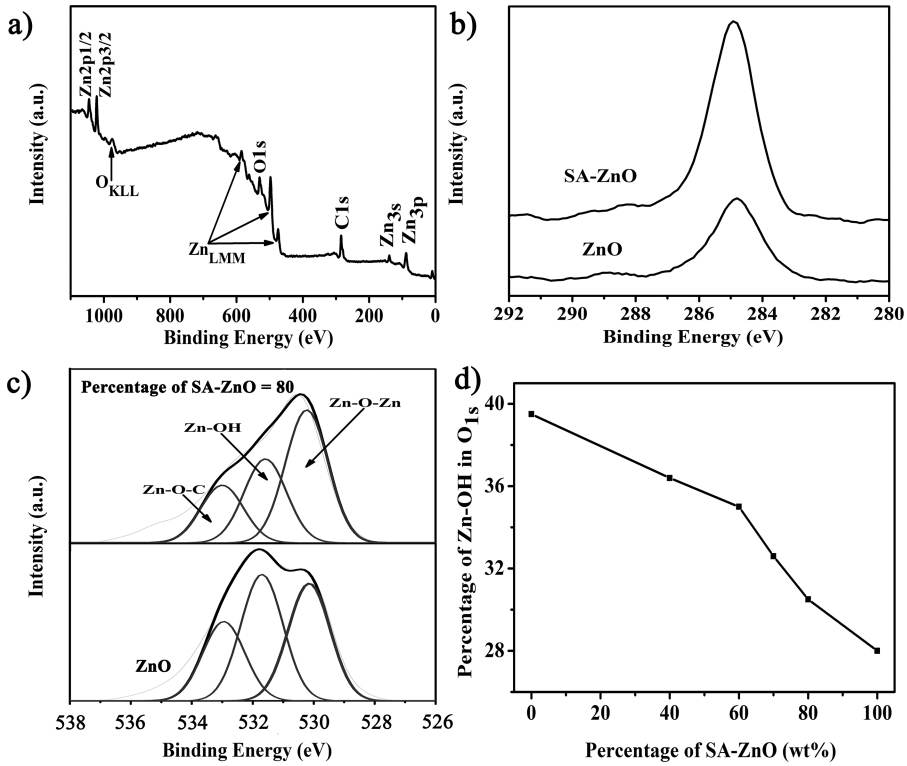

Figure 2. (a) XPS survey spectrum on the surface prepared with the percentage of SA-ZnO = 70. (b) High-solution C 1s XPS spectra of the initial ZnO surface and the SA-ZnO surface. (c) High-solution O 1s XPS spectra of the initial ZnO surface and the ZnO surface prepared with the percentage of SA-ZnO = 80. (d) Dependence of the Percentage of Zn−OH in O 1s on the percentage of SA-ZnO.

max-2400) with Cu Kα radiation. Field emission scanning electron microscopy (FE-SEM, Zeiss) was used to investigate the surface morphology of the as-prepared surfaces. The surface chemical composition of the as-prepared samples was analyzed on a PHI-5702 electron spectrometer using Mg Kα radiation as the excitation source and the binding energies were referenced to the C 1s at 284.80 eV. The water contact angles (CAs) and sliding angles were measured using a SL200KB apparatus by injecting 5 μL of water droplets onto the as-prepared surfaces. Each water CA and sliding angle was an average value of at least five measurements on different locations of the surface. The contact angle hysteresis (CAH) was calculated by the difference between measured values of the advancing and receding contact angles. The adhesive forces of superhydrophobic surfaces were measured using a high sensitivity micro-electromechanical balance

dx.doi.org/10.1021/am5015937 | ACS Appl. Mater. Interfaces 2014, 6, 8868−8877

system (Dataphysics DCAT 11, Germany) with a charge coupled device (CCD) camera. Water droplet of 5 μL was suspended on a metal ring first, and the superhydrophobic surface was placed on the balance table. Then, the superhydrophobic surface was moved upward at a constant speed of 0.02 mm s^{-1} in an ambient environment with a relative humidity of about 30%. Finally, the superhydrophobic surface began to move downward once in contact with the microdroplet, while the balance force gradually increased until reached the maximum. The maximum force when the surface is just leaving the water droplet is defined as the adhesive force.

3. RESULTS AND DISCUSSION

Superhydrophobic ZnO surfaces with tunable water adhesion were fabricated by the subsequent introduction of roughness and low energy surface via a spray-coating deposition of a mixture containing both hydrophobic and hydrophilic ZnO NPs. Figure 1a shows the XRD pattern of the as-prepared surfaces, indicating that all diffraction peaks could be assigned to ZnO with a hexagonal structure (JCPDS No: 36-1451). Figure 1b shows the IR spectra of hydrophilic ZnO, hydrophobic SA-ZnO NPs, and stearic acid. The carbonyl stretch of stearic acid at around 1702 cm^{-1} in IR spectrum disappeared in the sample of SA-ZnO.[53] Simultaneously, new peaks emerged at around 1540 and 1465 cm^{-1} are attributed to $m(COO)_{asym}$ and $m(COO)_{sym}$, respectively,[54] resulting from the formation of stearate. Disappearance of the peak at around 1702 cm^{-1} and emergency of the two peaks at around 1540 and 1465 cm^{-1} clearly indicated that the chemical reaction took place between ZnO and stearic acid. However, there was no evidence of these above-mentioned peaks in the spectrum of hydrophilic ZnO NPs. Thus, it can be reasonably concluded that ZnO NPs were successfully modified with stearic acid. Figure 1c,d shows FE-SEM images of ZnO NP surfaces with low and high magnifications, respectively. The low-magnification FE-SEM image exhibits that the ZnO NPs randomly cover the desired substrate (Figure 1c). In the high-magnification FE-SEM image, the ZnO NPs ranged in size from below 100 nm to several hundred nanometers were relatively aggregated, resulting in numerous void spaces and nanometer-scale roughness, which affected its superhydrophobicity.

To achieve the heterogeneous chemical composition on the surfaces, the mass percentage of hydrophobic SA-ZnO NPs in the hydrophobic/hydrophilic ZnO NP mixtures was adjusted. The heterogeneous chemical composition of the as-prepared ZnO NP surfaces is analyzed by XPS. Figure 2a shows the XPS survey spectrum of the surface prepared with the mass percentage of SA-ZnO = 0.7; it can be seen that the elements Zn, O, and C are detected for the surface. From the high-resolution XPS spectra for C 1s (Figure 2b), it can be observed that the intensity of C 1s peak at 284.8 eV apparently increased, compared with that of pure ZnO NPs. To get more information on the changes of the surface compositions, we collected the high-resolution XPS data of O 1s peak for the ZnO surfaces prepared with the percentage of SA-ZnO = 80 and 0 (pure ZnO), respectively (Figure 2c). It can be seen that multielement spectra of O 1s centered at 532.9, 531.6, and 530.2 eV was fitted to Zn−O−C, Zn−OH, and Zn−O−Zn, respectively. When the percentage of SA-ZnO is increased from 0 to 80, the surfaces present a decrease on the relative amount of oxygen in hydroxyl groups (Zn−OH) from 39.5% to 30.3%. What is worthy of more attention is that the amount of surface hydroxyl group (Zn−OH) is decreased with increasing the percentage of SA-ZnO in the hydrophobic/hydrophilic ZnO NPs mixture (Figure 2d). On the basis of the above analysis, it can be concluded that we can control the surface composition by changing the percentage of hydrophobic SA-ZnO NPs in the hydrophobic/hydrophilic ZnO NP mixtures.

The wettability of the as-prepared ZnO surfaces has been studied by CA measurements. From Figure 3a, it can be seen

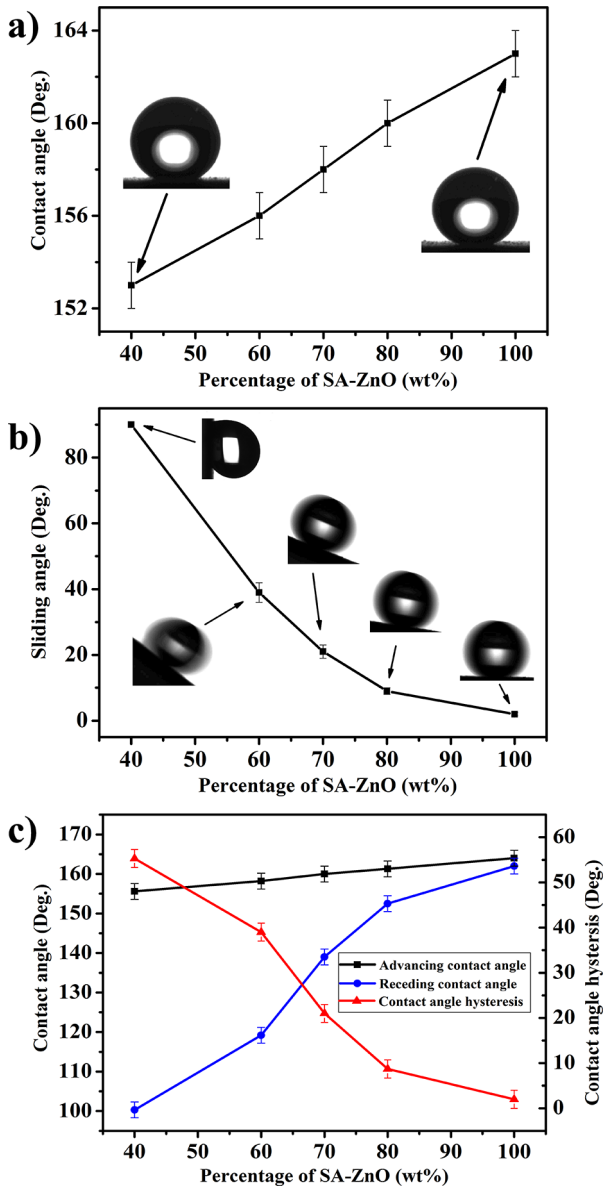

Figure 3. Dependence of (a) water contact angle and (b) sliding angle on the percentage of SA-ZnO. (c) Dependence of advancing contact angle, receding contact angle, and contact angle hysteresis on the percentage of SA-ZnO. Insets are the shapes of water droplets (5 μL) on the related surfaces.

that the five types of ZnO surfaces have the similar superhydrophobicity with CAs higher than 150°. Such high hydrophobicity can be ascribed to the combined effect of the low surface energy materials and the microstructures on the surface. In this work, given that the similarity of the surface morphologies of the ZnO samples, it can be therefore concluded that the chemical composition plays a decisive role in determining the surface wettability and adhesion. As the percentage of SA-ZnO is decreased from 100 to 40, more hydrophilic hydroxyl groups would exist on the ZnO surfaces,

dx.doi.org/10.1021/am5015937 | ACS Appl. Mater. Interfaces 2014, 6, 8868−8877

thus resulting in a decrease of the water CAs on the rough ZnO surfaces from 163 ± 1° to 153 ± 1° as well as an increase of the water sliding angles from 2 ± 1° to 9 ± 1°, 21 ± 2°, 39 ± 3°, and 90° (insets in Figure 3b). We also investigated the contact angle hysteresis (CAH) for the droplets on the surfaces; it can be seen that the water CAH increases with a decrease in the percentage of SA-ZnO (Figure 3c), and different water CAH would lead to different dynamic performances of the droplets.[55] Consequently, the water adhesion on the superhydrophobic ZnO surfaces can be controlled by simply changing the percentage of SA-ZnO in the ZnO NP mixtures.

Different water adhesions (or sliding angles) mean the surfaces with different adhesive forces, by using a high-sensitivity microelectromechanical balance system, the adhesive force of the as-prepared surfaces were measured accurately. Figure 4a exhibits typical CCD images of the process, in which the water droplet was slightly distorted under the drag of the surface prepared with the percentage of SA-ZnO = 80 after its contact with the microdroplet, and the adhesive force is denoted as the measured value when the surface totally departed from the microdroplet. Figure 4b shows the changes of adhesive force for the superhydrophobic ZnO surfaces prepared with different percentage of SA-ZnO. It is obvious that the adhesive force of the as-prepared surface can be adjusted from extremely low (~2.5 μN) to very high (~111.6 μN) as the percentages of SA-ZnO is decreased from 100 to 40 (Figure 4c).

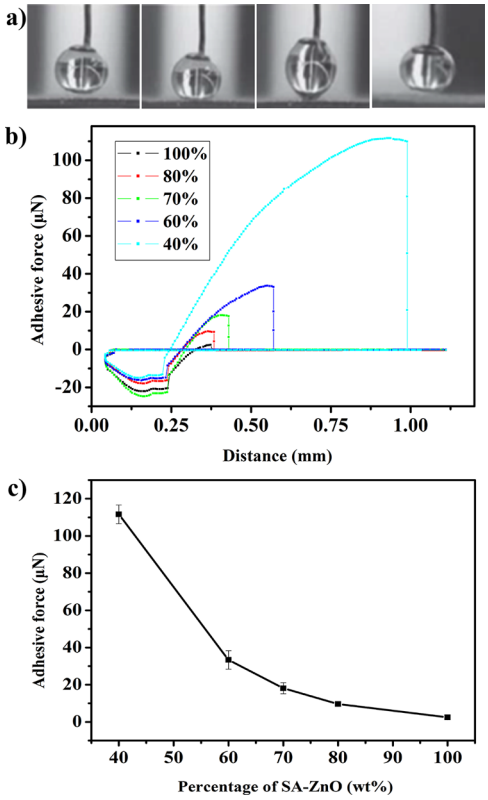

Figure 4. Dynamic adhesion measurement on the as-prepared surface: (a) CCD images for a typical measurement process. The surface prepared with the percentage of SA-ZnO = 80 is slight contact with a water droplet of 5 μL and then allowed to relax. (b) Force−distance curves on the superhydrophobic surfaces prepared with the percentage of SA-ZnO = 100, 80, 70, 60, and 40. (c) Dependence of the adhesive force on the percentage of SA-ZnO.

The as-prepared superhydrophobic surfaces have excellent tunable adhesive properties and can be used in the selective transportation of microdroplets with different volumes. As shown in Figure 5, two microdroplets with different volumes (left, 6 μL; right, 3 μL) were firstly placed on the low adhesive superhydrophobic surface prepared with pure SA-ZnO (Figure 5a). The two microdroplets were then touched by the medium adhesive surface prepared with the percentage of SA-ZnO = 60, which was placed above the low adhesive surface (Figure 5b). Due to the medium adhesive force, only the microdroplet of 3 μL stuck to the medium adhesive surface with the microdroplet of 6 μL stayed on the low adhesive surface (Figure 5c). Hence, by using the as-prepared medium adhesive superhydrophobic surfaces, the microdroplet of 3 μL can be stuck selectively and transferred from the low adhesive surface to the desired surface successfully (Figure 5d). It is the forces acting on the microdroplets that determine whether the microdroplets could be lifted or maintained motionless. In this system, the gravitational force on the microdroplet and the adhesive force between the microdroplet and the surface are regarded as primary forces. If the adhesive force of the medium adhesive surface is larger than the sum of the gravitational force of the water droplet and the adhesive force of the low adhesive surface, the microdroplet would stick to the medium adhesive superhydrophobic surface prepared with the percentage of SA-ZnO = 60 (the upper surface in Figure 5). Otherwise, it would stay on the initial low adhesive surface. In our experiment, the microdroplet of 3 μL was stuck to the medium adhesive surface, because the adhesive force of the medium adhesive surface (33.5 μN) is larger than the sum of the gravitational force of the 3 μL water droplet (about 29.4 μN) and the adhesive force of the low adhesive surface (2.5 μN). For the microdroplet of 6 μL with higher gravitational force (the gravitational force is about 58.8 μN), the results are opposite. These results illuminate that the selective transportation of microdroplets can be realized in order to satisfy requirements in practice just by controlling the adhesive force of the smart surfaces.

Five types of superhydrophobic ZnO surfaces with different sliding angles of 2 ± 1°, 9 ± 1°, 21 ± 2°, 39 ± 3°, and 90° have been fabricated by a facile spray-coating process. It was reported that whether a water droplet is pinned on or rolls off

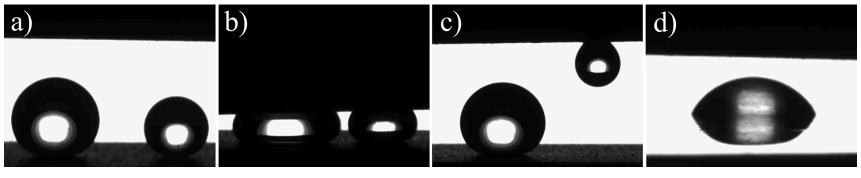

Figure 5. Process for the selective transportation of microdroplets (a) with different volumes (left, 6 μL; right, 3 μL) on the low adhesive surface. (b,c) Contacting the two water droplets with the medium adhesive superhydrophobic ZnO surface and the 3 μL droplet was selectively adhered with the 6 μL droplet unchanged. (d) Transferring the 3 μL droplet toward the hydrophilic surface.

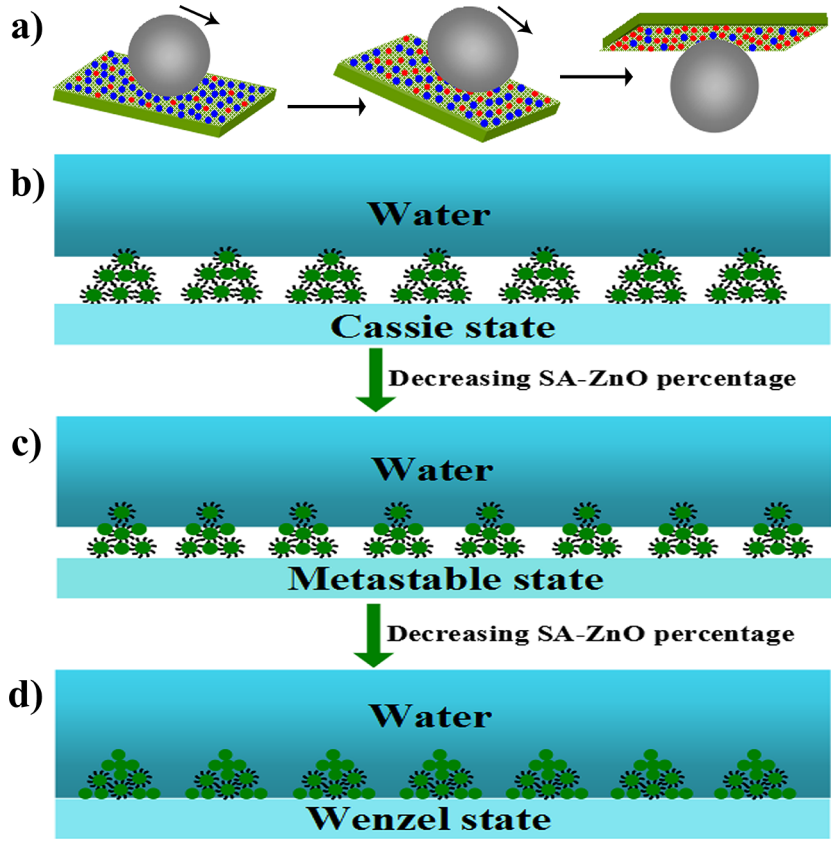

Figure 6. Schematic illustration of liquid–solid contact modes: (a) as the percentage of SA-ZnO is decreased, the liquid–solid contact mode is changed from the Cassie state, metastable state to the Wenzel state (the blue and red dots represent hydrophobic and hydrophilic ZnO NPs, respectively); (b) when the percentage of SA-ZnO is high, the water droplets are suspended by the gas layers trapped at the microscales and the water droplets would reside in the Cassie state on the superhydrophobic textured surface, thus, the adhesion of the surface is extremely low and the water droplets easily roll off with the surface slightly tilted; (c) decreasing the percentage of SA-ZnO, the water droplets may partially wet superhydrophobic surfaces with air trapped in the valleys (such a liquid–solid contact mode is part way between the Cassie and the Wenzel modes, is called the metastable state), thus, the adhesion of the surface is between that of the above two modes and the water droplets roll off with the surface significantly tilted; (d) further decreasing the percentage of SA-ZnO, the water droplets fully penetrate the grooves of the superhydrophobic surface and the water droplets would reside in the Wenzel state, thus the surface possesses high adhesion that could pin the water droplets on the surface without any movement.

the superhydrophobic surface is ascribed to the distinct contact modes (the Cassie state, the metastable state, and the Wenzel state). In addition, the superhydrophobic wetting state can be artificially controlled between the Cassie state with low adhesion to the Wenzel state with high adhesion through changing the chemical composition of a surface or its microstructure.[11,30] In this work, the chemical composition is the main factor that influences the adhesion, due to the analogous surface morphologies of all the ZnO samples. Thus, the water adhesion on the same superhydrophobic ZnO surface could be effectively tuned through controlling chemical composition of the surfaces without altering the surface morphology by changing the percentage of SA-ZnO (Figure 6a). When the superhydrophobic surface is prepared with high percentage of SA-ZnO (100, 80), the larger percentage of hydrophobic molecules dramatically decreases the adhesion of the water droplet on the superhydrophobic surface, leading to the Cassie state (Figure 6b). As the percentage of SA-ZnO is decreased to 70 and 60, more hydrophilic hydroxyl groups would exist on the ZnO surfaces and the water droplet may partially wet the superhydrophobic surface with air trapped in the valleys to form the metastable state (Figure 6c). Further decreasing the percentage of SA-ZnO to 40, hydrophilic ZnO NPs become denser and more hydrogen bonds would be produced, and the water droplet completely fills the valleys of the sueprhydrophobic surface to form the Wenzel state (Figure 6d). From above, it can be found that the superhydrophobic states can be tuned from the low adhesive Cassie state to the medium high adhesive metastable state and the high adhesive Wenzel state through regulating the surface chemical composition without altering the microstructures, which is controlled by decreasing the percentage of SA-ZnO through the spray-coating process.

It is reported that a wetting transition depends either on the way that the droplet is put onto a surface or on surface geometry.[56,57] In our work, it is also possible that surface composition will result in a wetting transition after the external pressure is applied on the medium and high adhesive superhydrophobic surfaces. In the compression experiment, water droplets of 8 μL were first placed on the surfaces with different water adhesion prepared with different percentages of SA-ZnO. Then the water droplets were compressed by the low adhesive superhydrophobic ZnO surface obtained by pure SA-ZnO NPs from above with a certain pressure. The applied pressure during compression can be simply calculated by the Laplace equation ($\Delta P = 4\gamma|\cos\theta|/d$, $d < 1$ mm, d represents the

dx.doi.org/10.1021/am5015937 | ACS Appl. Mater. Interfaces 2014, 6, 8868–8877

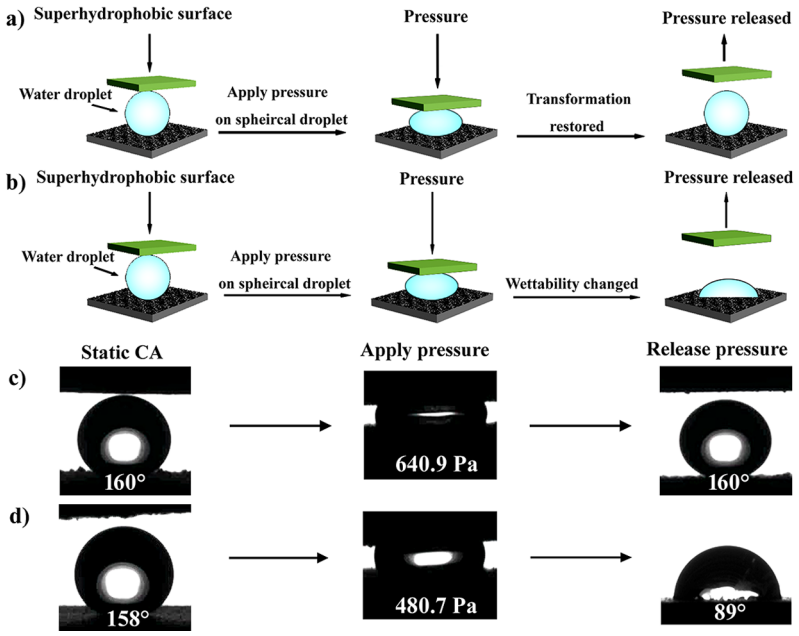

Figure 7. Schematic illustration of pressure induced water droplet wettability (a) unchanged on the low adhesive superhydrophobic surfaces (percentages of SA-ZnO = 100, 80) and (b) water droplet wettability changes from superhydrophobicity to hydrophilicity on the medium and high adhesive superhydrophobic surfaces (percentages of SA-ZnO = 70, 60, and 40); (c) and (d) are the corresponding digital images of water droplet on the low (percentage of SA-ZnO = 80) and medium (percentage of SA-ZnO = 70) adhesive superhydrophobic surfaces before and after application of external pressure.

distance between the low adhesive superhydrophobic surface and the surface bearing water droplet, γ is the surface tension of the water droplet and the surface tension of water (here, it is 72.1 mN/m), and θ, which is close to 180°, is the critical CA at the final position when the pressure is applied). It is observed that water droplets are expanded and distorted obviously with an increase in contact area under the applied pressure. Subsequently, the pressure was released (Figure 7a,b). After release of the applied pressure, the wetting transition between superhydrophobicity and hydrophilicity cannot or can be achieved depending on the adhesive property of the superhydrphobic surface, which is determined by the densities of the hydrophilic hydroxyl groups on the ZnO surfaces. When the droplets on the low adhesive superhydrophobic surface prepared by the percentage of SA-ZnO = 80 are under the compression test (Figure 7c), water CA was almost unvaried after being compressed by the applied pressure of 640.9 Pa, even if being distorted badly under the compression procedure (see the Supporting Information, Figure S1). In fact, water droplets were extruded out of the superhydrophobic surface more than once during the experiment. However, if an external pressure of 480.7 Pa was applied between the droplet and the medium adhesive superhydrophobic surface (the percentage of SA-ZnO = 70), the droplet wouldn't round up again and the water CA decreases from 158° to about 89° (Figure 7d). The dynamic wetting behavior of a pressed water droplet on superhydrophobic surfaces prepared with the percentages of SA-ZnO = 100, 60, and 40 was also demonstrated (see the Supporting Information, Figure S2). In our experiment, the wetting transition after the external pressure is applied was closely related to the surface composition (the density of hydrophilic hydroxyl group on ZnO surfaces). When the water droplets on the low adhesive superhydrophobic surfaces (the contact mode is the Cassie state) prepared with the percentages of SA-ZnO = 100, 80 were pressured, water CA was almost unvaried after being compressed by the applied pressure, due to the low density of hydrophilic hydroxyl group on the ZnO surfaces (Figure 2d). With increasing the density of hydrophilic hydroxyl group on ZnO surfaces by decreasing the percentage of the SA-ZnO in the mixture ZnO NPs, water droplet wettability changes from superhydrophobicity to hydrophilicity on the medium adhesive superhydrophobic surfaces prepared with the percentages of SA-ZnO = 70, 60 (Figure 2d), this is due to the transition from the metastable state to the Wenzel state, because the action of pressure physically extrudes the underlying trapped air between the droplet and the solid surface.[26] With further increasing the density of hydrophilic hydroxyl group on ZnO surfaces, water droplet wettability also changes from superhydrophobicity to hydrophilicity on the high adhesive superhydrophobic surfaces (the contact mode is the Wenzel state) prepared with the percentage of SA-ZnO = 40 (Figure 2d), which is ascribed to dramatic increase of the surface contact area on the microstructure caused by external pressure. Thus, by changing the percentage of SA-ZnO in the hydrophobic/hydrophilic ZnO NP mixtures through the spray-coating process, the heterogeneous chemical composition on the tunable adhesive superhydrophobic ZnO surfaces with the different density of the hydrophilic hydroxyl group is obtained, and the surface composition results in a wetting transition after the external pressure is applied on the medium and high adhesive superhydrophobic surfaces.

The special ability of such surfaces with tunable adhesion to allow selective microdroplet transportation has potential in a wide range of applications, for example, in droplet-based microreactors. Recently, such droplet-based microreactor systems have exhibited significant advantages in protein crystallization, enzymatic kinetics, and some other biochemical reactions.[45,58] Taking advantage of the controlled adhesive forces of the superhydrophobic ZnO surfaces, we demonstrated the selective, step-by-step transportation of microdroplets

toward the quantitative detection of $AgNO_3$ and NaOH in the droplet-based microreactors. As shown in Figure 8a, two droplets were placed on the superhydrophobic surface with low adhesion to water: left, 6 μL of 0.15 mol L^{-1} $CuCl_2$, which was intended to be used in the detection of 6 μL of 0.3 mol L^{-1} $AgNO_3$; right, 3 μL of 0.15 mol L^{-1} $CuCl_2$, which was intended to be used in the detection of 3 μL of 0.3 mol L^{-1} NaOH. First, the two water droplets were contacted with the medium adhesive superhydrophobic surface and only the 3 μL of droplet was transferred from the low adhesive to the medium adhesive superhydrophobic surface, leaving the 6 μL of droplet unchanged (Figure 8b,c). Subsequently, the 3 μL of droplet was transported to be in contact with another 3 μL of droplet containing 0.3 mol L^{-1} NaOH on a stainless steel surface and deposited on the surface (Figure 8d,e,h,i). The two droplets coalesced after contact and blue $Cu(OH)_2$ was produced (Figure 8f,j). After transportation of 3 μL of $CuCl_2$ droplet, the high adhesive superhydrophobic ZnO surface was used to finish the chemical reaction for production of AgCl. Similarly, the 6 μL of 0.15 mol L^{-1} $CuCl_2$ droplet was touched and transported to the high adhesive superhydrophobic surface (Figure 8k,l,m). After contact, the two droplets coalesced and white AgCl was produced, due to the reaction between Ag^{+1} and Cl^{-1} (Figure 8n–s). In other words, by using the tunable adhesive superhydrophobic ZnO surfaces with different adhesive forces, the selective transportation of two droplets with different volumes was achieved, and applied in the droplet-based microreactor for the quantitative detection of $AgNO_3$ and NaOH.

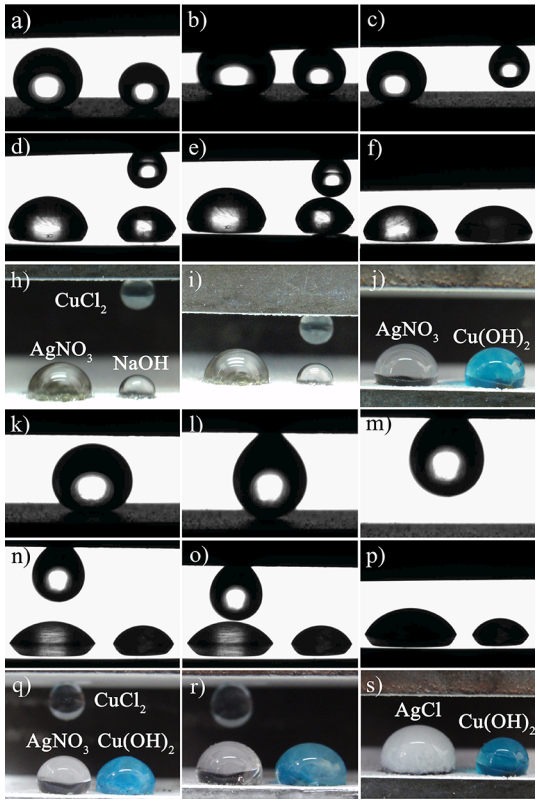

Figure 8. Applying the tunable adhesive superhydrophobic surfaces in the selective transportation of microdroplets with different volumes: (a) placing water droplets containing 0.15 mol L^{-1} of $CuCl_2$ on the low adhesive superhydrophobic surface (left, 6 μL; right, 3 μL); (b,c) contacting the two droplets with the medium adhesive superhydrophobic surface and the 3 μL droplet was selectively adhered with the 6 μL droplet unchanged; (d–j) coalescence of the 3 μL of 0.15 mol L^{-1} $CuCl_2$ droplet to another 3 μL of 0.3 mol L^{-1} NaOH droplet (right on a stainless steel surface), and the blue $Cu(OH)_2$ (right) was produced on the stainless steel surface; (k–m) contacting the 6 μL of 0.15 mol L^{-1} $CuCl_2$ droplet with the high adhesive superhydrophobic surface and transferring the 6 μL droplet from the low adhesive surface to the high adhesive surface; (n–s) coalescence of the 6 μL of 0.15 mol L^{-1} $CuCl_2$ droplet to another 6 μL of 0.3 mol L^{-1} $AgNO_3$ droplet (left on a stainless steel surface), and the white AgCl (left) was produced on the stainless steel surface.

Regarding the real application, the superhydrophobic property of the artifical superhydrophobic surfaces can be easily lost by mechanical contact such as abrasion because the man-made roughness of the superhydrophobic surfaces is extremely fragile. Unlike natural superhydrophobic plant leaves, the wrecked surfaces almost cannot be repaired automatically, which is a disaster to the artifical superhydrophobic surfaces. The facile spray-coating process allows the local repair at anytime, anywhere, and almost any substrate. As shown in Figure 9a, after the superhydrophobic surfaces prepared with the percentage of SA = 70 scratched with a knife, the water CA decreases sharply to about 105°. To repair the destroyed superhydrophobic surfaces, we only need to spray the mixed ZnO NP suspensions on the wrecked surface again. The reparative surfaces can restore its good superhydrophobicity with the water CA of 158° and adhesive property with the water sliding angle of 21 ± 2° (Figure 9b). What is more, the time of regeneration and the number of repairable times are limitless on any substrate. The simple repairability of superhydrophobicity is an attractive feature from the viewpoint of the utilization of superhydrophobic surfaces.

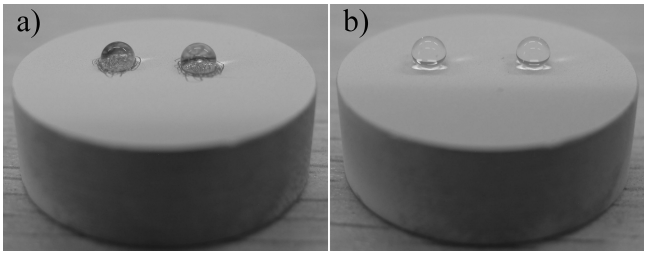

Figure 9. Photographs of water droplets (a) on the superhydrophobic ZnO surface partly destroyed by a knife and (b) on the regenerated superhydrophobic ZnO surface.

4. CONCLUSIONS

In conclusion, tunable adhesive superhydrophobic ZnO surfaces have been fabricated successfully by a facile spray-coating process based on the design of heterogeneous chemical composition on the ZnO NP surfaces. By simply changing the percentages of SA-ZnO in hydrophobic/hydrophilic ZnO NP mixtures, tunable adhesive superhydrophobic ZnO surfaces have been fabricated successfully. Compared with the conventional tunable adhesive superhydrophobic surfaces, the water adhesion on the as-prepared superhydrophobic ZnO surfaces has been tuned effectively. On the basis of the different adhesive forces of the tunable adhesive superhydrophobic surfaces, the selective transportation of microdroplets with different volumes was achieved for the first time. Moreover, the dynamic wetting behavior of a pressed water droplet on different adhesive superhydrophobic surfaces is demonstrated,

and the wetting transition between superhydrophobicity and hydrophilicity cannot or can be achieved on the tunable adhesive superhydrophobic surfaces depending on the adhesive property of the surfaces, which is determined by the density of the hydrophilic hydroxyl group on the ZnO surfaces. In addition, we demonstrated a proof of selective transportation of microdroplets with different volumes for application in the droplet-based microreactors via our tunable adhesive superhydrophobic surfaces for the quantitative detection of $AgNO_3$ and NaOH. Last but not least, scratches on the surface could be repaired by spraying the mixed ZnO NPs suspension again on the wrecked surface, and the superhydrophobicity and adhesive property of the surfaces can be regenerated simultaneously. Meanwhile, the selective transportation of droplets with different volumes was realized by using the tunable adhesive superhydrophobic ZnO surfaces, and we propose that such tunable adhesive superhydrophobic surfaces could also be potentially useful in many applications, such as microfluidic devices, selective water droplet transportation, and droplet-based bioseparation.

■ ASSOCIATED CONTENT

Ⓢ Supporting Information

A series of images showing a compression experiment with a water droplet on the low adhesive superhydrophobic surface prepared with the percentage of SA-ZnO = 80; corresponding optical images of wettability unchanged and changed surface on the different adhesive superhydrophobic surfaces before and after application of external pressure. This material is available free of charge via the Internet at http://pubs.acs.org.

■ AUTHOR INFORMATION

Corresponding Authors

*J. Li. Tel.: +86 931 7971533. E-mail: lijian@licp.cas.cn.

*Z. Lei. Tel.: +86 931 7970359. E-mail: leizq@nwnu.edu.cn.

Notes

The authors declare no competing financial interest.

■ ACKNOWLEDGMENTS

The National Nature Science Foundation of China (Grant No. 21301141), the program for Changjiang Scholars and Innovative Research Team in University, China (IRT1177), and the Scientific and Technical Innovation Project of Northwest Normal University (NWNU-LKQN-12-6) are financially supporting this work.

■ REFERENCES

(1) Liu, K.; Yao, X.; Jiang, L. Recent Developments in Bio-inspired Special Wettability. *Chem. Soc. Rev.* **2010**, *39*, 3240−3255.

(2) Ou, J.; Hu, W.; Xue, M.; Wang, F.; Li, W. Superhydrophobic Surfaces on Light Alloy Substrates Fabricated by a Versatile Process and Their Corrosion Protection. *ACS Appl. Mater. Interfaces* **2013**, *5*, 3101−3107.

(3) Min, W. L.; Jiang, B.; Jiang, P. Bioinspired Self-Cleaning Antireflection Coating. *Adv. Mater.* **2008**, *20*, 3914−3918.

(4) Howarter, J. A.; Youngblood, J. P. Self-Cleaning and Anti-Fog Surfaces via Stimuli-Responsive Polymer Brushes. *Adv. Mater.* **2007**, *19*, 3838−3843.

(5) Li, J.; Yan, L.; Ouyang, Q.; Zha, F.; Jing, Z.; Li, X.; Lei, Z. Facile Fabrication of Transparent Superamphiphobic Coating on Paper to Prevent Liquid Pollution. *Chem. Eng. J.* **2014**, *246*, 238−243.

(6) Wang, Y.; Xue, J.; Wang, Q.; Chen, Q.; Ding, J. Verification of Icephobic/Anti-icing Properties of a Superhydrophobic Surface. *ACS Appl. Mater. Interfaces* **2013**, *5*, 3370−3381.

(7) Zhang, S.; Lu, F.; Tao, L.; Liu, N.; Gao, C.; Feng, L.; Wei, Y. Bio-Inspired Anti-Oil-Fouling Chitosan-Coated Mesh for Oil/Water Separation Suitable for Broad pH Range and Hyper-Saline Environments. *ACS Appl. Mater. Interfaces* **2013**, *5*, 11971−11976.

(8) Ju, J.; Xiao, K.; Yao, X.; Bai, H.; Jiang, L. Bioinspired Conical Copper Wire with Gradient Wettability for Continuous and Efficient Fog Collection. *Adv. Mater.* **2013**, *25*, 5937−5942.

(9) Shirtcliffe, N. J.; McHale, G.; Newton, M. I.; Zhang, Y. Superhydrophobic Copper Tubes With Possible Flow Enhancement and Drag Reduction. *ACS Appl. Mater. Interfaces* **2009**, *1*, 1316−1323.

(10) Li, J.; Liu, X.; Ye, Y.; Zhou, H.; Chen, J. Gecko-Inspired Synthesis of Superhydrophobic ZnO Surfaces with High Water Adhesion. *Colloids Surf., A* **2011**, *384*, 109−114.

(11) Liu, M.; Zheng, Y.; Zhai, J.; Jiang, L. Bioinspired Super-antiwetting Interfaces with Special Liquid-Solid Adhesion. *Acc. Chem. Res.* **2010**, *43*, 368−377.

(12) Barthlott, W.; Neinhuis, C. Purity of the Sacred Lotus, or Escape from Contamination in Biological Surfaces. *Planta* **1997**, *202*, 1−8.

(13) Li, X. M.; Reinhoudt, D.; Crego-Calama, M. What do We Need for a Superhydrophobic Surface? A Review on the Recent Progress in the Preparation of Superhydrophobic Surfaces. *Chem. Soc. Rev.* **2007**, *36*, 1350−1368.

(14) Feng, L.; Li, S.; Li, Y.; Li, H.; Zhang, L.; Zhai, J.; Song, Y.; Liu, B.; Jiang, L.; Zhu, D. Super-Hydrophobic Surfaces: From Natural to Artificial. *Adv. Mater.* **2002**, *14*, 1857−1860.

(15) Feng, L.; Zhang, Y.; Xi, J.; Zhu, Y.; Wang, N.; Xia, F.; Jiang, L. Petal Effect: A Superhydrophobic State with High Adhesive Force. *Langmuir* **2008**, *24*, 4114−4119.

(16) Jin, M.; Feng, X.; Feng, L.; Sun, T.; Zhai, J.; Li, T.; Jiang, L. Superhydrophobic Aligned Polystyrene Nanotube Films with High Adhesive Force. *Adv. Mater.* **2005**, *17*, 1977−1981.

(17) Li, J.; Liu, X.; Ye, Y.; Zhou, H.; Chen, J. A facile Solution-Immersion Process for the Fabrication of Superhydrophobic Surfaces with High Water Adhesion. *Mater. Lett.* **2012**, *66*, 321−323.

(18) Hong, X.; Gao, X.; Jiang, L. Application of Superhydrophobic Surface with High Adhesive Force in No Lost Transport of Superparamagnetic Microdroplet. *J. Am. Chem. Soc.* **2007**, *129*, 1478−1479.

(19) Cheng, Z.; Du, M.; Lai, H.; Du, Y.; Zhang, N.; Sun, K. Selective Transprortation of Microdroplets Assisted by a Superhydrophobic Surface with PH-Responsive Adhesion. *Chem.—Asian J.* **2013**, *8*, 3200−3206.

(20) Yong, J.; Chen, F.; Yang, Q.; Zhang, D.; Bian, H.; Du, G.; Si, J.; Meng, X.; Hou, X. Controllable Adhesive Superhydrophobic Surfaces Based on PDMS Microwell Arrays. *Langmuir* **2013**, *29*, 3274−3279.

(21) Ou, J.; Hu, W.; Li, C.; Wang, Y.; Xue, M.; Wang, F.; Li, W. Tunable Water Adhesion on Titanium Oxide Surfaces with Different Surface Structures. *ACS Appl. Mater. Interfaces* **2012**, *4*, 5737−5741.

(22) Zhao, X. D.; Fan, H. M.; Luo, J.; Ding, J.; Liu, X. Y.; Zou, B. S.; Feng, Y. P. Electrically Adjustable, Super Adhesive Force of a Superhydrophobic Aligned MnO_2 Nanotube Membrane. *Adv. Funct. Mater.* **2011**, *21*, 184−190.

(23) Cheng, Z.; Du, M.; Lai, H.; Zhang, N.; Sun, K. From Petal Effect to Lotus Effect: A Facile Solution Immersion Process for the Fabrication of Superhydrophobic Surfaces with Controlled Adhesion. *Nanoscale* **2013**, *5*, 2776−2783.

(24) Sun, T. L.; Qing, G. Y. Biomimetic Smart Interface Materials for Biological Applications. *Adv. Mater.* **2011**, *23*, H57−H77.

(25) Ren, H. X.; Chen, X.; Huang, X. J.; Im, M.; Kim, D. H.; Lee, J. H.; Yoon, J. B.; Gu, N.; Liu, J. H.; Choi, Y. K. A Conventional Route to Scalable Morphology-Controlled Regular Structures and Their Superhydrophobic/Hydrophilic Properties for Biochips Application. *Lab Chip* **2009**, *9*, 2140−2144.

(26) Lafuma, A.; Quéré, D. Superhydrophobic states. *Nat. Mater.* **2003**, *2*, 457−460.

(27) Bormashenko, E.; Pogreb, R.; Stein, T.; Whyman, G.; Erlich, M.; Musin, A.; Machavariani, V.; Aurbach, D. Characterization of Rough Surfaces with Vibrated Drops. *Phys. Chem. Chem. Phys.* **2008**, *10*, 4056−4061.

(28) Cassie, A. B. D.; Baxter, S. Wettability of Porous Surfaces. *Trans. Faraday Soc.* **1944**, *40*, 546−550.
(29) Wenzel, R. N. Resistance of Solid Surfaces to Wetting by Water. *Ind. Eng. Chem.* **1936**, *28*, 988−994.
(30) Bormashenko, E.; Pogreb, R.; Whyman, G.; Erlich, M. Resonance Cassie-Wenzel Wetting Transition for Horizontally Vibrated Drops Deposited on a Rough Surface. *Langmuir* **2007**, *23*, 12217−12221.
(31) Zheng, Y.; Gao, X.; Jiang, L. Directional Adhesion of Superhydrophobic Butterfly Wings. *Soft Matter* **2007**, *3*, 178−182.
(32) Lai, Y.; Gao, X.; Zhuang, H.; Huang, J.; Lin, C.; Jiang, L. Designing Superhydrophobic Porous Nnanostructures with Tunable Water Aadhesion. *Adv. Mater.* **2009**, *21*, 3799−3803.
(33) Li, J.; Liu, X.; Ye, Y.; Zhou, H.; Chen, J. Fabrication of Superhydrophobic CuO Surfaces with Tunable Water Adhesion. *J. Phys. Chem. C* **2011**, *115*, 4726−4729.
(34) Yong, J.; Chen, F.; Yang, Q.; Zhang, D.; Du, G.; Si, J.; Yun, F.; Hou, X. Femtosecond Laser Weaving Superhydrophobic Patterned PDMS Surfaces with Tunable Adhesion. *J. Phys. Chem. C* **2013**, *117*, 24907−24912.
(35) Zhao, X. D.; Fan, H. M.; Liu, X. Y.; Pan, H.; Xu, H. Y. Pattern-Dependent Tunable Adhesion of Superhydrophobic MnO_2 Nanostructured Film. *Langmuir* **2011**, *27*, 3224−3228.
(36) Zhang, Q.; Wang, J. A Simple Way to Achieve Tunable Adhesion in Superhydrophobic Nanostructured Co_3O_4 Films. *Mater. Lett.* **2013**, *108*, 267−269.
(37) Huang, X.; Kim, D.; Im, M.; Lee, J.; Yoon, J.; Choi, Y. "Lock-and-Key" Geometry Effect of Patterned Surfaces: Wettability and Switching of Adhesive Force. *Small* **2009**, *5*, 90−94.
(38) Zhang, D.; Chen, F.; Yang, Q.; Yong, J.; Bian, H.; Ou, Y.; Si, J.; Meng, X.; Hou, X. A Simple Way to Achieve Pattern-Dependent Tunable Adhesion in Superhydrophobic Surfaces by a Femtosecond Laser. *ACS Appl. Mater. Interfaces* **2012**, *4*, 4905−4912.
(39) Cheng, Z.; Gao, J.; Jiang, L. Tip Geometry Controls Adhesive States of Superhydrophobic Surfaces. *Langmuir* **2010**, *26*, 8233−8238.
(40) Li, J.; Jing, Z.; Yang, Y.; Yan, L.; Zha, F.; Lei, Z. A Facile Solution Immersion Process for the Fabrication of Superhydrophobic ZnO Surfaces with Tunable Water Adhesion. *Mater. Lett.* **2013**, *108*, 267−269.
(41) Lee, W.; Park, B. G.; Kim, D. H.; Ahn, D. J.; Park, Y.; Lee, S. H.; Lee, K. B. Nanostructure-Dependent Water-Droplet Adhesiveness Change in Superhydrophobic Anodic Aluminum Oxide Surfaces: From Highly Adhesive to Self-Cleanable. *Langmuir* **2010**, *26*, 1412−1415.
(42) Hu, Z.; Li, W. Preparation of Superhydrophobic Fe_2O_3 Nanorod Films with the Tunable Water Adhesion. *J. Colloid Interface Sci.* **2012**, *376*, 245−249.
(43) Li, J.; Jing, Z.; Yang, Y.; Zha, F.; Yan, L.; Lei, Z. Reversible Low Adhesive to High Adhesive Superhydrophobicity Transition on ZnO Nanoparticle Surfaces. *Appl. Surf. Sci.* **2014**, *289*, 1−5.
(44) Darmanin, T.; Guittard, F. Highly Hydrophobic Films with Various Adhesion by Electrodeposition of Poly(3,4-bis(alkoxy)-thiophene)s. *Soft Matter* **2013**, *9*, 1500−1505.
(45) Cheng, Z.; Hou, R.; Du, Y.; Lai, H.; Fu, K.; Zhang, N.; Sun, K. Designing Heterogeneous Chemical Composition on Hierarchical Structured Copper Substrates for the Fabrication of Superhydrophobic Surfaces with Controlled Adhesion. *ACS Appl. Mater. Interfaces* **2013**, *5*, 8753−8760.
(46) Lai, Y.; Lin, C.; Huang, J.; Zhuang, H.; Sun, L.; Nguyen, T. Markedly Controllable Adhesion of Superhydrophobic Spongelike Nanostructure TiO_2 Films. *Langmuir* **2008**, *24*, 3867−3873.
(47) Wang, M.; Chen, C.; Ma, J.; Xu, J. Preparation of Superhydrophobic Cauliflower-like Silica Nanospheres with Tunable Water Adhesion. *J. Mater. Chem.* **2011**, *21*, 6962−6967.
(48) Kakade, B. A. Chemical Control of Superhydrophobicity of Carbon Nanotube Surfaces: Droplet Pinning and Electrowetting Behavior. *Nanoscale* **2013**, *5*, 7011−7016.
(49) Zhao, N.; Xie, Q.; Kuang, X.; Wang, S.; Li, Y.; Lu, X.; Tan, S.; Shen, J.; Zhang, X.; Zhang, Y.; Xu, J.; Han, C. C. A Novel Ultra-Hydrophobic Surface: Statically Non-Wetting but Dynamically Non-Sliding. *Adv. Funct. Mater.* **2007**, *17*, 2739−2745.
(50) Seo, J.; Lee, S.; Han, H.; Chung, Y.; Lee, J.; Kim, S. D.; Kim, Y. W.; Lim, S.; Lee, T. Reversible Wettability Control of Silicon Nanowire Surfaces: From Superhydrophilicity to Superhydrophobicity. *Thin Solid Films* **2013**, *527*, 179−185.
(51) Wu, W.; Wang, X.; Liu, X.; Zhou, F. Spray-Coated Fluorine-Free Superhydrophobic Coatings with Easy Repairability and Applicability. *ACS Appl. Mater. Interfaces* **2009**, *1*, 1656−1661.
(52) Li, J.; Wan, H.; Ye, Y.; Zhou, H.; Chen, J. One-Step Process for the Fabrication of Superhydrophobic Surfaces with Easy Repairability. *Appl. Surf. Sci.* **2012**, *258*, 3115−3118.
(53) Wang, S. T.; Feng, L.; Jiang, L. One-Step Solution-Immersion Process for the Fabrication of Stable Bionic Superhydrophobic Surfaces. *Adv. Mater.* **2006**, *18*, 767−770.
(54) Li, J.; Liu, X.; Ye, Y.; Zhou, H.; Chen, J. A Simple Solution-Immersion Process for the Fabrication of Superhydrophobic Cupric Stearate Surface with Easy Repairable Property. *Appl. Surf. Sci.* **2011**, *258*, 1772−1775.
(55) Yüce, M. Y.; Demirel, A. L.; Menzel, F. Tuning the Surface Hydrophobicity of Polymer/Nanoparticle Composite Films in the Wenzel Regime by Composition. *Langmuir* **2005**, *21*, 5073−5078.
(56) Patankar, N. A. Transition Between Superhydrophobic States on Rough Surfaces. *Langmuir* **2004**, *20*, 7097−7102.
(57) Bhushan, B.; Nosonovsky, N. Biomimetic Superhydrophobic Surfaces: Multiscale Approach. *Nano Lett.* **2007**, *7*, 2633−2637.
(58) Song, H.; Chen, D. L.; Ismagilov, R. F. Reactions in Droplets in Microfluidic Channels. *Angew. Chem., Int. Ed.* **2006**, *45*, 7336−7356.